First publ. in: Physical Review Letters 89 (2007) 8, 083001

Isomer-Resolved Ion Spectroscopy

Roland Fromherz,[1] Gerd Ganteför,[1] and Alexandre A. Shvartsburg[2,*]
[1]*Fachbereich Physik, Universität Konstanz, 78457 Konstanz, Germany*
[2]*Division of Chemistry, National Center for Toxicological Research, HFT-233, Jefferson, Arkansas 72079*

We demonstrate the isomer-resolved spectroscopy of gas-phase ions, with different geometries separated prior to spectroscopic probe using ion mobility techniques. Specifically, ring and chain isomers of carbon cluster anions with 10–12 atoms have been separated by ion mobility/mass spectrometry and examined by photoelectron spectroscopy. This methodology should also apply to other ion spectroscopies, including IR photodissociation.

PACS numbers: 33.60.–q, 36.40.–c, 39.30.+w, 39.90.+d

Over the past two decades, novel ion sources [1,2] have revolutionized gas-phase physical chemistry. A plethora of cluster ions were characterized by mass spectrometry, and their physical and chemical properties were measured [3–6]. However, explanation of these properties was often elusive because the underlying geometries remained unknown. Structural elucidation of cluster ions proved an inordinate difficulty. In the 1990's, isolation of fullerenes [7] that were first discovered in ion beams [8] had made understanding the growth of free clusters topical.

Historically, spectroscopy was the primary tool to characterize gaseous molecules. Though application of classical optical spectroscopies to molecular ions is impeded by low signal intensity caused by miniscule target density, other spectroscopic methods (photoelectron spectroscopy, PES [9–17] and IR photodissociation spectroscopy [18,19]) have proven useful. In PES, anions are photoexcited above the detachment threshold, and the kinetic energy of released electrons is measured. This reveals the electronic structure of neutrals at the anion geometry. In IR photodissociation, vibrational modes excited by IR absorption are revealed via cluster dissociation. Calculations for reasonable candidate geometries then enable the structural assignment [16,19]. However, a major difficulty [9,12,17] is that ion sources routinely produce isomeric mixtures, with compositions sensitive in a convoluted manner to minute design and operational details. For example, C_n anions have more than one isomer for all $n \geq 10$, including monocyclic rings and chains for $n = 10$–50, monocyclic and polycyclic rings for $n = 20$–60, and fullerenes and rings for $n > 30$ [9,20–23]. Similarly, multiple isomers were identified for S_n^- [17], Si_n^-/Si_n^+ with $n \geq 17$ [15,24] and Sn_n^+ with $n \geq 18$ [25]. Hence, the measured spectrum is often a superposition of spectra for each isomer and does not represent any geometry [9]. Further, different geometries have unequal photoabsorption efficiencies; hence, the weighing factors for individual spectra superimposed would not normally match isomer abundances. Disentangling the features from different geometries and those from different transitions in the same geometry is, generally, a challenge. In practice, finite experimental resolution commonly makes the spectra of isomeric mixtures featureless; PES of large Si_n anions is an example [26].

Here, we report the development of isomer-resolved spectroscopy, where a gas-phase isomeric ion mixture is separated prior to a spectroscopic probe. This is achieved by coupling a spectroscopic (here PES) instrument to ion-mobility spectroscopy (IMS). IMS is a method to separate and characterize the isomers of gas-phase molecular ions [20]. It involves timing the motion of an ion pulled by an electric field through an inert buffer gas. The measured drift velocity can be converted into the diffusion constant (mobility) that is inversely proportional to the orientationally averaged collision integral (cross section). The collision integrals determined by IMS can be related to specific geometries via calculations of varying sophistication [27–29]. This methodology has successfully characterized the clusters of C [21,23], Si [30,31], Ge [32], and Sn [25,33], all exhibiting multiple isomers.

A new IMS/PES instrument (Fig. 1) has been built on the PES platform described previously [34]. Briefly, clusters are generated in a pulsed arc source (PACIS) operated at 20 Hz and cooled in an extender of 17 cm length and 4–6 mm diameter. In the original design, anions were passed through a 5-cm field-free region, injected into a time-of-flight (TOF) mass spectrometer, and crossed a Nd:YAG (4.66 eV, 20 Hz) laser beam. The detached electrons were collected and energy-dispersed using a ''magnetic bottle'' electron spectrometer. An IMS drift tube has now been installed between source and TOF. This 14-cm long copper tube consists of a stack of seven concentric rings with the internal diameter of 6.7 cm and two terminal plates featuring 3–5 mm apertures. Metal pieces are separated by 70-μm thick mylar gaskets that seal off the tube interior, and are connected by resistors. The tube is held together by insulated steel bolts that fix all parts to the central ring. This ring features an insulating support that mounts the tube on the chamber floor and two gas lines: one for the buffer gas inflow, the other connected to a Pirani vacuum transducer for pressure measurement. The temperature is monitored by several thermocouples affixed along the drift

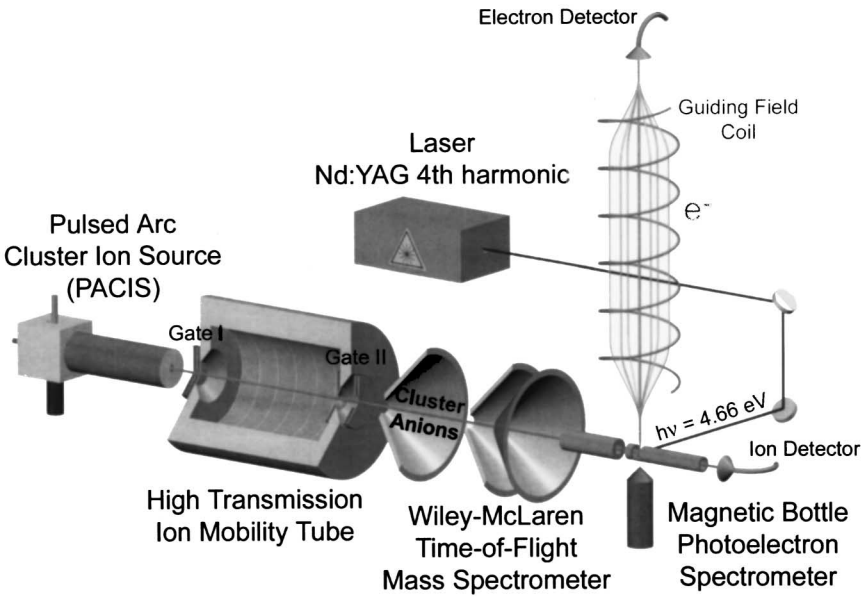

FIG. 1. Schematic diagram of the new IMS/TOF/PES instrument.

tube. Ion packets entering the tube are formed using a gate immediately preceding the entrance plate, where the potential on a copper ring oscillates between −40 and 17 V. The stopping potential of −40 V with respect to the grounded PACIS source suffices to exclude all anions from the tube. At the potential of 17 V, a rectangular pulse of 5–10 μs duration penetrates inside. Ions then travel through the drift tube under the influence of a near-uniform electric field of $D = 12.5$ V/cm along the axis, created by a voltage of 165 V applied across the tube and partitioned by the resistor chain. Ions exiting the tube through an aperture in the end plate encounter another gate analogous to that mounted on the front plate and enter the TOF mass spectrometer. The time delay between the two gates sets the mobility of the ions registered in the mass spectrum and, hence, in the photoelectron spectrum.

Present experiments were performed using He buffer gas at a temperature of 300 K and pressure of $P = 0.43$ Torr. The latter is below ~3–5 Torr typical for the injected-ion drift tube IMS [20,23,25]. This is because the apertures in this tube are much wider than in the earlier setups (~0.2–0.4 mm). Wide apertures are needed here to reduce ion losses in IMS to the level ensuring a sufficient signal for the PES analysis; still the measured transmission efficiency is ~2% only. This necessitates a lower pressure inside, or else the escaping buffer gas would flood the vacuum chamber and TOF mass spectrometer. As a consequence of low pressure inside the tube, the voltage across had to be limited to preserve a reasonable E/P ratio allowing proper IMS operation. This has constrained the instrumental mobility resolution that is proportional to $E^{-1/2}$. Still, the electric field was high enough to move the IMS conditions out of the low drift field regime, where the mobility is field independent [23]. Hence, the mobilities measured here should not be compared to zero-field quantities [20–23]. Under these conditions, we had (per each ion pulse) ~100 isomer-resolved mass-selected anions in the laser beam focus, with ~10 electrons collected. Performing IMS in a high-field regime causes substantial collisional heating of drifting ions. Steady-state temperatures may be estimated using the ''two-temperature treatment'' [23]. For example, the temperature of the C_{10}^- chain (the mobility in He at 300 K is $8 \times 10^{-4} V^{-1} s^{-1} m^2$ [23]) would be ~800 K.

To validate the capability of this technique to measure isomer-resolved spectra, we revisited C_n anions with $n =$ 10–12: perhaps the best-studied polymorphic cluster system. For $n \leq 9$, all C_n^- are linear chains [20,23]. Monocyclic rings first appear at $n = 10$, and their relative abundance tends to increase with increasing n. Chain and ring geometries could be separated in injected-drift tube IMS for all sizes [20,23]. The arrival time distributions measured in this instrument using the ion signal (Fig. 2) qualitatively reproduce those published [20–23], though the exact mobilities differ as discussed above. (The temperatures at which rings and chains interconvert are not known, but must be above those of the drifting ions, else no isomers would separate.) Then total photoelectron spectra for the same species were measured with the drift tube inoperative. These spectra agree with the standard PES data [9,12,13]. For some C_n anions (e.g., $n = 11$ and 12), those data contain the spectra for both chains and rings, with the result depending on source conditions [9,12]. No experiments for $n \geq 13$ were attempted as the vertical detachment energy (VDE) of chains moves above the energy of a single Nd:YAG laser photon.

Having tested IMS and PES parts separately, we measured the photoelectron spectra for $n = 5$, 9–12 at specific

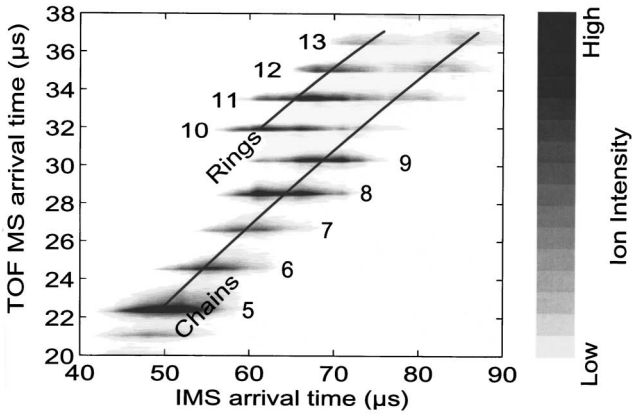

FIG. 2. IMS arrival time distributions measured for C_n anions ($n = 5$–13, ion signal). The appearance of ring geometries at shorter drift times for $n \geq 10$ is evident.

drift times, defined by setting the delay between the openings of entrance and exit gates. For each size studied, measured IMS arrival time distributions (Fig. 2) were scanned with a 2 μs step, providing about five spectra for each IMS peak. Spectra acquired for C_5^- and C_9^- [Fig. 3(a)] as a function of drift time are both identical to the standard PES references. This was expected since C_5^- and C_9^- have a single isomer, the chain. The situation for C_n anions with $n \geq 10$ is entirely different; the example of C_{11}^- is presented in Figs. 3(b) and 4. The photoelectron spectra for drift times under the two IMS peaks are quite distinct. Scans for the one at shorter times (monocyclic ring) have a major feature at the electron flight time of 2.5 μs (corresponding to an energy of $\sim$3 eV), while those for the one at longer drift times (chain) exhibit a peak at 4 μs (energy of $\sim$4 eV). These separated spectra match those expected [9] for the ring and chain, respectively. Their superposition duly produces the reference composite spectrum for C_{11}^- obtained using regular PES [Fig. 3(b)]. The results for C_{10}^- and C_{12}^- (Fig. 4) are similar.

Two key trends in the measured spectra are that the electron VDE (i) is always lower for ring compared to chain isomers and (ii) increases at higher n for both families. These could be understood by considering the development of molecular π orbitals that determine the HOMO, and, hence, the VDE [9,12]. A better delocalization of extra electron in larger systems generally lowers HOMO, thus increasing VDE. This engenders the effect (ii) and also (i), since the dimensions of chains exceed those of ring isomers. This pattern is not specific to clusters of carbon: similar trends were encountered for S_n^- chains and rings [17]. An even-odd alternation of VDE for both ring and chain C_n^- has been reported [9,12]; however, the interval of sizes studied is too narrow to characterize this (considering a significant thermal broadening of all PES features).

These findings demonstrate the ability of an ion-mobility spectrometry/photoelectron spectroscopy instrument to separate different ion geometries prior to a spectroscopic probe, thus obtaining isomer-resolved spectra. We have already mentioned semiconductor, tin, and sulfur clusters, where an IMS/PES capability would be of great help in structural characterization efforts. In another example, in high-resolution IMS the ''monocyclic ring'' feature for C_n anions with $n \geq 13$ actually contained two or more peaks [22]. These were tentatively assigned as true rings and rings with chains attached (''tadpoles''), but the mobilities computed for them did not fit the measurements [22,29]. Significantly different photoelectron spectra for rings and tadpoles should enable a clear identification of those peaks in IMS/PES. The practical utility of our first IMS/MS/PES implementation is limited by its modest mobility resolution and sensitivity. We anticipate that, with increasing resolving power and signal throughput, this technique would make a substantial impact on the structural characterization of gas-phase ions, cluster ions in particular [35]. The present demonstration of isomer-resolved PES should also stimulate efforts to couple IMS with other ion spectroscopy methods, such as IR photodissociation [18,19]. Furthermore, IMS is not merely an isomer separation utility, but a powerful structural tool by itself. Combining ion-mobility and spectroscopic data for

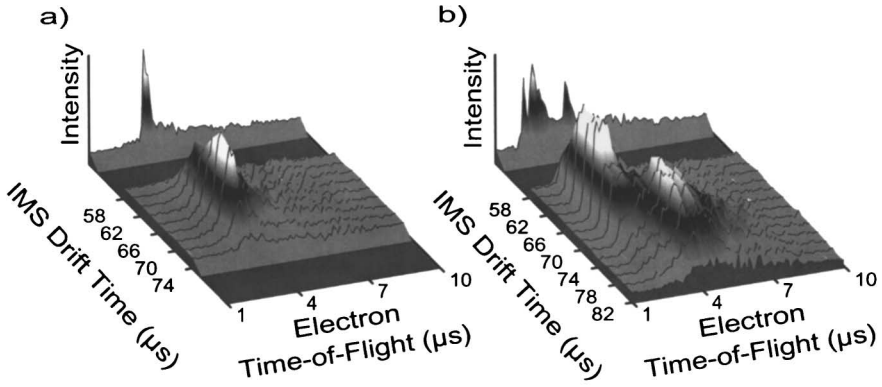

FIG. 3. Photoelectron spectra (time domain) measured for C_9 anion (a) and C_{11} anion (b) scanning across the drift time selected in the IMS stage. Scans acquired in the basic PES mode (without a drift tube) are plotted in the back for reference.

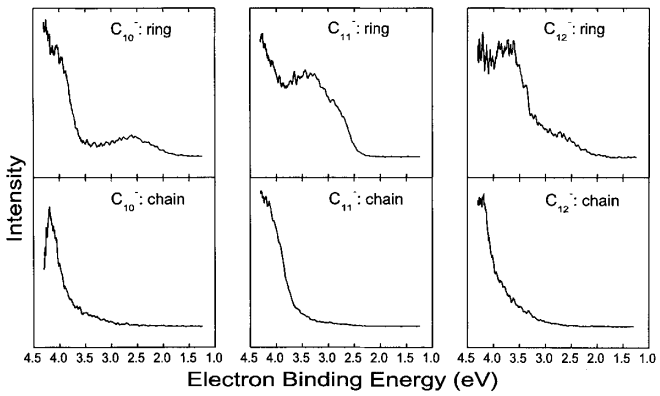

FIG. 4. Photoelectron spectra (energy domain, averages of $\sim 10^4$–10^5 laser shots) measured for C_{10}, C_{11}, and C_{12} anions at the drift times corresponding to the monocyclic ring (top) and linear chain (bottom). Scans were composed by integrating traces at several drift times under the respective peaks in IMS data.

the same system should substantially improve access to the structures of gas-phase ions.

Much inspiration for this work originated from discussions with M. F. Jarrold. We thank J. R. Chelikowsky, K. M. Ho, K. A. Jackson, and G. Seifert for their useful advice on the PES of carbon clusters. Funding from the Deutsche Forschungsgemeinschaft is gratefully acknowledged.

*Corresponding author.
Email address: ashvartsburg@nctr.fda.gov

[1] V. E. Bondybey and J. H. English, J. Chem. Phys. **74**, 6978 (1981).
[2] M. Yamashita and J. B. Fenn, J. Phys. Chem. **88**, 4451 (1984).
[3] S. K. Loh, D. A. Hales, L. Lian, and P. B. Armentrout, J. Chem. Phys. **90**, 5466 (1989).
[4] Q. L. Zhang, Y. Liu, R. F. Curl, F. K. Tittel, and R. E. Smalley, J. Chem. Phys. **88**, 1670 (1988).
[5] M. F. Jarrold, J. E. Bower, and K. Creegan, J. Chem. Phys. **90**, 3615 (1989).
[6] K. Fuke, K. Tsukamoto, F. Misaizu, and M. Sanekata, J. Chem. Phys. **99**, 7807 (1993).
[7] W. Kratschmer, L. D. Lamb, K. Fostiropoulos, and D. R. Huffman, Nature (London) **347**, 354 (1990).
[8] H. W. Kroto, J. R. Heath, S. C. O'Brien, R. F. Curl, and R. E. Smalley, Nature (London) **318**, 162 (1985).
[9] S. Yang, K. J. Taylor, M. J. Craycraft, J. Conceicao, C. L. Pettiette, O. Chesnovsky, and R. E. Smalley, Chem. Phys. Lett. **144**, 431 (1988).
[10] G. Ganteför, K. H. Meiwes-Broer, and H. O. Lutz, Phys. Rev. A **37**, 2716 (1988).
[11] D. W. Arnold, S. E. Bradforth, T. N. Kitsopoulos, and D. M. Neumark, J. Chem. Phys. **95**, 8753 (1991).
[12] M. Kohno, S. Suzuki, H. Shiromaru, T. Moriwaki, and Y. Achiba, Chem. Phys. Lett. **282**, 330 (1998).
[13] H. Handschuh, G. Ganteför, B. Kessler, P. S. Bechthold, and W. Eberhardt, Phys. Rev. Lett. **74**, 1095 (1995).
[14] S. Ogut and J. R. Chelikowsky, Phys. Rev. B **55**, R4914 (1997).
[15] J. Müller, B. Liu, A. A. Shvartsburg, S. Ogut, J. R. Chelikowsky, K. W. M. Siu, K. M. Ho, and G. Ganteför, Phys. Rev. Lett. **85**, 1666 (2000).
[16] X. B. Wang, X. Yang, J. B. Nicholas, and L. S. Wang, Science **294**, 1322 (2001).
[17] G. Ganteför, S. Hunsicker, and R. O. Jones, Chem. Phys. Lett. **236**, 43 (1995).
[18] M. Weber, J. A. Kelley, S. B. Nielsen, P. Ayotte, and M. A. Johnson, Science **287**, 2461 (2000).
[19] G. Gregoire, J. Velasquez, and M. A. Duncan, Chem. Phys. Lett. **349**, 451 (2001).
[20] G. Von Helden, P. R. Kemper, N. G. Gotts, and M. T. Bowers, Science **259**, 1300 (1993).
[21] N. G. Gotts, G. von Helden, and M. T. Bowers, Int. J. Mass Spectrom. Ion Process. **149/150**, 217 (1995).
[22] Ph. Dugourd, R. R. Hudgins, J. Tenenbaum, and M. F. Jarrold, Phys. Rev. Lett. **80**, 4197 (1998).
[23] A. A. Shvartsburg, G. C. Schatz, and M. F. Jarrold, J. Chem. Phys. **108**, 2416 (1998).
[24] R. R. Hudgins, M. Imai, Ph. Dugourd, and M. F. Jarrold, J. Chem. Phys. **111**, 7865 (1999).
[25] A. A. Shvartsburg and M. F. Jarrold, Phys. Rev. A **60**, 1235 (1999).
[26] M. Maus, G. Ganteför, and W. Eberhardt, Appl. Phys. A **70**, 535 (1999).
[27] A. A. Shvartsburg and M. F. Jarrold, Chem. Phys. Lett. **261**, 86 (1996).
[28] A. A. Shvartsburg, B. Liu, M. F. Jarrold, and K. M. Ho, J. Chem. Phys. **112**, 4517 (2000).
[29] A. A. Shvartsburg, B. Liu, K. W. M. Siu, and K. M. Ho, J. Phys. Chem. A **104**, 6152 (2000).
[30] K. M. Ho, A. A. Shvartsburg, B. Pan, Z. Y. Lu, C. Z. Wang, J. G. Wacker, J. L. Fye, and M. F. Jarrold, Nature (London) **392**, 582 (1998).
[31] I. Rata, A. A. Shvartsburg, M. Horoi, T. Frauenheim, K. W. M. Siu, and K. A. Jackson, Phys. Rev. Lett. **85**, 546 (2000).
[32] A. A. Shvartsburg, B. Liu, Z. Y. Lu, C. Z. Wang, M. F. Jarrold, and K. M. Ho, Phys. Rev. Lett. **83**, 2167 (1999).
[33] A. A. Shvartsburg, R. R. Hudgins, Ph. Dugourd, and M. F. Jarrold, Chem. Soc. Rev. **30**, 26 (2001).
[34] C. Y. Cha, G. Ganteför, and W. Eberhardt, Rev. Sci. Instrum. **63**, 5661 (1992).
[35] One way to increase the IMS resolving power is to cool the buffer gas, as the resolution is proportional to $(\text{temperature})^{1/2}$. In IMS/PES, this would simultaneously improve the PES resolution, by reducing the thermal broadening of PES features apparent in the data.